

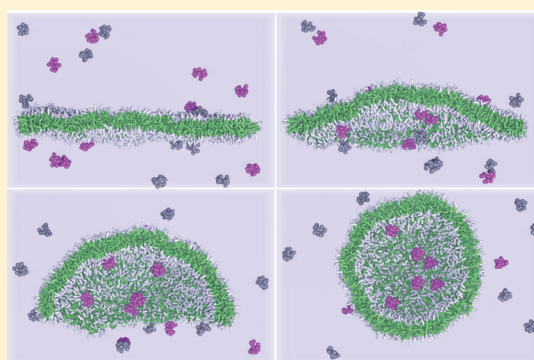
# On Protein Crowding and Bilayer Bulging in Spontaneous Vesicle Formation

Bram van Hoof,<sup>†,‡</sup> Albert J. Markvoort,<sup>†,‡</sup> Rutger A. van Santen,<sup>‡,§</sup> and Peter A. J. Hilbers<sup>\*,†,‡</sup>

<sup>†</sup>Department of Biomedical Engineering, <sup>‡</sup>Institute for Complex Molecular Systems, and <sup>§</sup>Department of Chemical Engineering and Chemistry, Technische Universiteit Eindhoven, P.O. Box 513, 5600 MB Eindhoven, The Netherlands

## S Supporting Information

**ABSTRACT:** Spontaneous aggregation of lipids into bilayers and vesicles is a key property for the formation of biological membranes. Understanding the compartmentalization achieved by vesicle formation is an important step toward understanding the origin of life, and is crucial in current efforts to develop artificial life. Spontaneously formed vesicles may be applied as artificial cells if they can efficiently encapsulate biomacromolecules. Recent studies report an enhanced concentration of encapsulated proteins during vesicle formation. In order to obtain more insight into this encapsulation process, here we simulate the spontaneous transition of flat bilayers to vesicles in the presence of solvated model proteins using molecular dynamics simulations. In the bilayer–vesicle transition, which is found to be unaffected by the presence of the solvated proteins, the bilayer edge remains at almost the same height, while the center of the membrane bulges out, a molecular pathway we denominate “bilayer bulging”. This bulging results in an interior protein concentration that is significantly lower than that of the solution. By means of an increased protein–membrane interaction, enhanced encapsulation of proteins inside the vesicles could be achieved in our simulations.



## INTRODUCTION

The spontaneous aggregation of lipids into bilayers and vesicles (liposomes) is an important property of one of the key components of biological cells, the cell membrane.<sup>1–6</sup> Therefore, compartmentalization achieved by vesicle formation is an important key to understanding the origin of life,<sup>7,8</sup> and plays an essential role in current efforts to develop artificial cells.<sup>9–11</sup> Their ability to encapsulate DNA,<sup>12</sup> RNA,<sup>13</sup> proteins,<sup>14</sup> or other biomacromolecules<sup>15</sup> is an important condition for the use of these vesicles as artificial cells.

In recent studies of the use of vesicles as artificial cells, Luisi and co-workers show an enhanced entrapment of proteins in vesicle formation, a so-called protein crowding effect.<sup>16,17</sup> In particular, using vesicles to entrap the complete ribosomal machinery for the enhanced green fluorescent protein, they find a 20-fold larger concentration of the molecular components of the machinery inside several of the vesicles. A similar phenomenon is observed with the entrapment of ferritin in spontaneously forming vesicles.<sup>18</sup> To explain the formation of vesicles with a highly enlarged concentration of proteins, Luisi suggests a mechanism involving competition between vesicle closure and solute capture rates. According to this hypothesis, empty vesicles close rapidly, but under the influence of adsorption of proteins to the membrane, this closure can be slowed down, allowing the accumulation of other solute molecules inside the closing vesicle.

The spontaneous formation of lipid vesicles has not only received the attention of experimentalists, but also molecular

simulations have frequently been employed to investigate such vesicles.<sup>19–21</sup> In the literature, vesicle formation is studied at the molecular level using a broad range of different simulation techniques, including dissipative particle dynamics, Brownian dynamics and molecular dynamics.<sup>4,22–26</sup> Although it is possible to investigate vesicle behavior with atomistic detail,<sup>25</sup> studies investigating the bilayer–vesicle transition have used a coarse grained representation in view of the large time and length scales required. The kinetics of the vesicle formation have been studied,<sup>4,22,26</sup> as well as the influence of the membrane composition on these kinetics.<sup>23,24</sup> However, the molecular details of the effect of proteins on vesicle formation have not yet been investigated in simulations.

Here, we employ molecular dynamics simulations to investigate the spontaneous formation of vesicles in the presence of solvated proteins, using our previously described coarse grained (CG) lipid model, which is a generic model that captures the behavior of a broad range of fatty acids and phospholipids.<sup>4</sup> Using an extended version of our CG model, we analyze the dynamics of the spontaneous formation of vesicles, both in the presence and absence of proteins. To this end, we extend our model with a generic water-soluble protein composed of identical particles. With this model, we test whether the molecular mechanisms of the spontaneous

Received: June 25, 2012

Revised: September 11, 2012

Published: October 1, 2012

bilayer–vesicle formation offer a possible explanation for the experimentally observed enhanced protein concentration. Furthermore, the influence of the strength of the adhesive forces between proteins and membrane on the vesicle formation and on the degree of encapsulation of proteins inside the vesicles is investigated.

## METHODS

**Molecular Dynamics Simulations.** The simulations have been performed in parallel employing either 1 node of 32 processors or 3–8 nodes of 4 processors on a Rocks Cluster, using the in-house molecular dynamics code PumMa.<sup>4</sup> A time step of 25 fs is used. A Berendsen thermostat and barostat are used to maintain a constant temperature of 307 K and a constant pressure of 1.0 atm, respectively. All nonbonded interactions are cut off at 1.2 nm in order to speed up the calculations. To prevent a drift in the linear momentum, the initial velocities are chosen such that the linear momentum is zero; also, every 1000 iterations, the velocities are corrected to restore the linear momentum to zero.

The force field consists of three types of interaction potentials, representing bonds, angles, and nonbonded interactions. An overview of the used bonded and nonbonded interaction potentials as well as of the used parameters is given in the Supporting Information.

**Coarse Grained Model.** The model employed in this work is an extension of the model used previously to study the behavior of phospholipid vesicles,<sup>4,27,28</sup> transmembrane proteins,<sup>29,30</sup> and self-reproduction of fatty acid vesicles.<sup>31</sup> In the previous model, three types of particles are present: W particles that represent water, T particles that represent the apolar fatty acid tails, and H particles that represent the fatty acid headgroups. In the extended model, a new particle type, P, is introduced to form the water-soluble proteins. As shown in Figure 1A, the water is represented by single particle W molecules, whereas fatty acids are represented by the H<sub>2</sub>T<sub>4</sub> molecule, and the water-soluble proteins are represented by the P<sub>17</sub> molecule, which is composed of 17 P particles bound together in a dendrimeric structure, with 1 center particle, 4 particles in the first layer bound to the center particle, and 12 particles in the second layer, 3 of which are bound to each particle of the first layer.

The interaction parameters for the W and H<sub>2</sub>T<sub>4</sub> molecules are taken from previous work by Markvoort et al.<sup>31</sup> To study the role of solvated proteins in the formation of vesicles, the model protein (P<sub>17</sub>) needs to be water-soluble. Therefore, the nonbonded interactions for the P particles are identical to those for W particles. The bond and angle interactions in the P<sub>17</sub> molecule are chosen to maintain a globular molecular structure. The P–H interaction is varied to represent different degrees of protein–membrane association, as specified in the next section. Importantly, due to the purely repulsive P–T interaction, protein insertion into the membrane is energetically highly unfavorable. Furthermore, protein aggregation is discouraged by setting the P–P interaction equal to the P–W and W–W interactions.

**Adsorption of Proteins to the Membrane.** To test the effect of the protein–membrane interaction on the protein concentration inside vesicles, the protein–headgroup interaction has to be varied. To that end, the P–H interaction is first evaluated in a system containing a solvated periodic fatty acid bilayer and 24 proteins randomly distributed across the solvent. An example of such a system is shown in Figure 1B. The

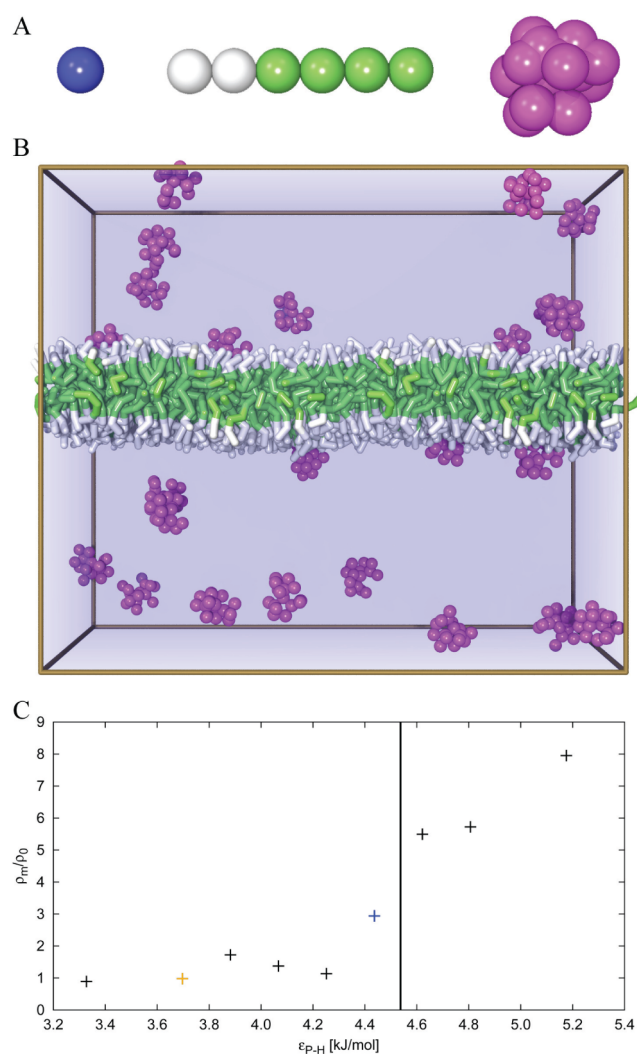


**Figure 1.** (A) Illustration of the different CG molecules. The CG water consists of a single W particle (blue); fatty acids are represented by a linear molecule built of two hydrophilic H particles (white) and four hydrophobic T particles (green); water-soluble proteins are represented by the P<sub>17</sub> molecule (magenta). (B) The periodic fatty acid bilayer with 24 solvated proteins used to measure the adsorption of proteins to the membrane as a function of the P–H interaction strength. (C) The relative protein density near the membrane  $\rho_m/\rho_0$  as a function of the protein–membrane interaction  $\epsilon_{P-H}$ , where  $\rho_m$  is the protein density within 1.2 nm of the membrane and  $\rho_0$  is the overall protein density in the water phase. The values for  $\epsilon_{P-H}$  selected for vesicle formation simulations (*vide infra*) are highlighted in orange and blue, respectively. The vertical line indicates the interaction strength beyond which no dissociation is observed ( $\epsilon_{P-H} \geq 4.62$  kJ mol<sup>−1</sup>).

periodic bilayer is 21.8 by 18.8 nm<sup>2</sup>, whereas the height of the periodic simulation box is 23.0 nm. Simulations of 25 ns are performed, where the first 2.5 ns are discarded to allow equilibration of the proteins across the simulation box. In these simulations, the association and dissociation behavior of the proteins is studied through systematic variation of the P–H interaction ( $\epsilon_{P-H} = 3.33, 3.70, 3.88, 4.07, 4.25, 4.44, 4.62, 4.81$ , and 5.18 kJ mol<sup>−1</sup>).

In simulations with  $\epsilon_{P-H} \leq 4.44$  kJ mol<sup>−1</sup>, the proteins disperse throughout the box, occasionally display association to the membrane, and then dissociate again. The protein density near the membrane is defined as  $\rho_m/\rho_0$ , where  $\rho_m$  is the protein density within 1.2 nm of the membrane (because the cutoff

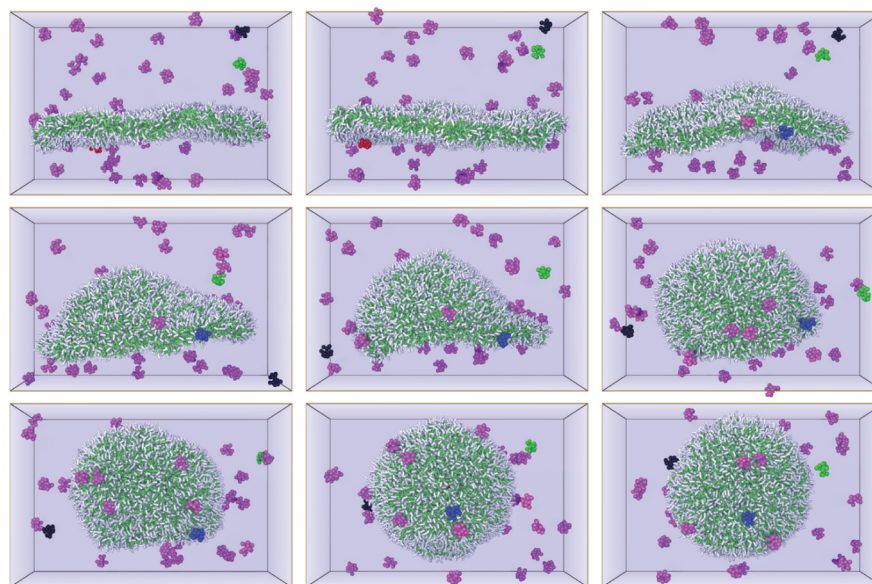


**Figure 2.** Snapshots of a representative simulation from the Associated series with frames shown every 5 ns, ordered from left to right and from top to bottom. The fatty acids are shown in a licorice representation; the proteins are shown in a spheres representation, with individual species colored in black, red, green, and blue, whereas the other 36 species are colored in magenta. For visibility, the water is not shown explicitly but is instead represented by a continuous blue opaque solvent.

radius for nonbonded interactions is 1.2 nm) and  $\rho_0$  is the overall protein density in the water phase. This protein density appears to have a positive correlation with the interaction strength of the protein particles with the fatty acid headgroups (see Figure 1C). However, for  $\epsilon_{p-H} \geq 4.62 \text{ kJ mol}^{-1}$ , the proteins never dissociate within the length of this simulation, once they are associated with the membrane. Therefore, those values for  $\epsilon_{p-H}$  are considered too large to use in our vesicle formation simulations, as an equilibrium distribution of the proteins would not be achieved within the time scale of these simulations. The value of  $\epsilon_{p-H} = 3.70 \text{ kJ mol}^{-1}$  is chosen to represent a neutral protein–membrane interaction, whereas  $\epsilon_{p-H} = 4.44 \text{ kJ mol}^{-1}$  is used to represent membrane-associated proteins.

**Simulations of Vesicle Formation.** The transition of a flat bilayer to a vesicle is studied. To create the initial configurations, first a periodic fatty acid bilayer is simulated for 88 ns to equilibrate. Subsequently, a circular patch with a radius of 17 nm is cut out from the bilayer and surrounded by water in a rectangular water box of 24 by 37 by 37 nm<sup>3</sup>. As a control, a basic configuration without proteins is simulated (labeled “Control”). Twelve copies of this basic configuration are created, with different initial velocities in each system.

Systems containing solvated proteins are constructed from the basic configuration without proteins. Each of these systems contains 40 proteins, which are inserted in the water phase. In the “Neutral” series, consisting of 24 individual simulations with  $\epsilon_{p-H} = 3.70 \text{ kJ mol}^{-1}$ , the proteins are distributed uniformly in the water phase, in accordance with the equilibrated protein distribution found with the periodic fatty acid bilayer. In the “Associated” series (24 simulations), the protein density within 1.2 nm of the circular bilayer patch is 50% higher than in the bulk of the water phase, to mimic the increased protein concentration found in the periodic bilayer simulations. A fourth series of 12 simulations, “NeutralPlus”, is performed employing the initial configurations with an increased protein density near the bilayer (as described for the “Associated”

series) but using the P–H interaction from the “Neutral” series. Each system is simulated 12 or 24 times, and each simulation is performed using different randomly assigned initial velocities and randomly inserted proteins in the water phase. In each simulation, the solvent and the proteins, when present, are allowed to equilibrate for 2.5 ns while keeping the fatty acid membrane fixed. Subsequently, the membrane is released and an unconstrained molecular dynamics simulation is performed.

## RESULTS

Simulations of vesicle formation are performed for the four different simulation series as described in the Methods section. In the first series, labeled “Control”, proteins are absent; a second series, with water-soluble model proteins, is called “Neutral”; the third series, denoted as “NeutralPlus”, contains the same proteins as in the Neutral series but with an enhanced initial protein density close to the membrane; in the fourth series, labeled “Associated”, proteins having an enhanced protein–membrane interaction are employed. All simulations display the successful formation of a single vesicle with a radius of 8.7 nm (measured at the interface between the two membrane leaflets), containing  $1.2 \times 10^4$  water molecules. An example of such a simulation is shown in Figure 2, where four proteins are highlighted with a different color: the green protein diffuses without contact with the membrane; both the blue and the black protein display a transient adhesion to the membrane, which does not lead to encapsulation; the red protein adheres to the membrane and is subsequently encapsulated, and, therefore, blocked from view after the second frame in the figure.

In Figure 3, the histograms of the number of encapsulated proteins in the “Neutral” and “Associated” series are shown. From the figure, it is clear that the protein–membrane interaction ( $\epsilon_{p-H}$ ) has a large effect on the protein concentration inside the vesicles. Given the volume of the formed vesicles, the expected amount of proteins inside the vesicles is 2.2 for an even protein concentration inside and



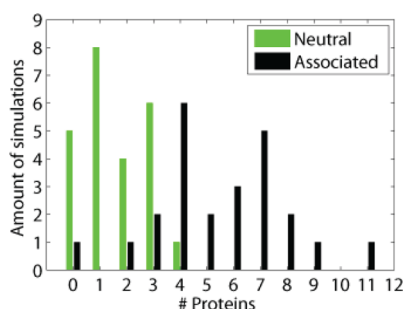


**Figure 3.** Histograms of the number of encapsulated proteins found in the simulations of the “Neutral” and “Associated” series.

outside the vesicle. Several vesicles, especially of the “Neutral” series, however, do not contain any proteins despite the relatively high bulk concentration. In contrast, enhanced encapsulation of proteins inside the vesicles, up to 5 times the bulk concentration, is observed for the “Associated” series, with an interior concentration larger than that of the bulk in 22 out of 24 simulations.

The effect of the protein–membrane interaction is also visible from Table 1, where the average amounts of proteins

**Table 1. Overview of the Average Simulation Results in the Four Different Vesicle Formation Simulation Series**

series	# sims	$\epsilon_{p-H}$ (kJ mol <sup>-1</sup> )	$\rho_m/\rho_0$ @ $t = 0$	# proteins	closure time (ns)
Control	12				
Neutral	24	3.70	1.0	$1.6 \pm 1.2$	$30.9 \pm 3.0$
NeutralPlus	12	3.70	1.5	$1.7 \pm 1.5$	$28.8 \pm 3.3$
Associated	24	4.44	1.5	$5.5 \pm 2.4$	$30.4 \pm 2.7$

enclosed in the vesicle are shown for all four series. In the Neutral series, the concentration is below the bulk concentration, with an average of 1.6 encapsulated proteins, or only 73% of the protein concentration in the bulk. The NeutralPlus series shows that this result is independent of the initial concentration near the membrane, as there the average number of proteins in the vesicle is 1.7, still much smaller than the bulk concentration. A significantly enlarged protein concentration is found in the Associated series, with an average of 5.5 proteins per vesicle, indicating that a specific protein–membrane interaction could suffice to obtain an enhanced entrapment of proteins in vesicles.

Table 1 also shows that the average vesicle closure time is almost identical in each of the four series, which suggests no influence of the present model proteins on the mechanisms behind the observed vesicle closure process. This is also seen when comparing the curvature of the membrane as a function of the simulation time in Figure 4A (the Supporting Information contains the method used to calculate the membrane curvature).

To elucidate the molecular mechanisms of the vesicle formation process as observed in our simulations, we inspect the trajectory from the Associated series in Figure 2. It is observed that the open side of the vesicle remains at almost the same height in the box, whereas the closed part of the vesicle membrane moves upward as the simulation proceeds, a pathway which we denominate “bilayer bulging”. This appears to be the case in all four simulation series, as shown in Figure 4C by plotting the maximal and minimal height of the fatty

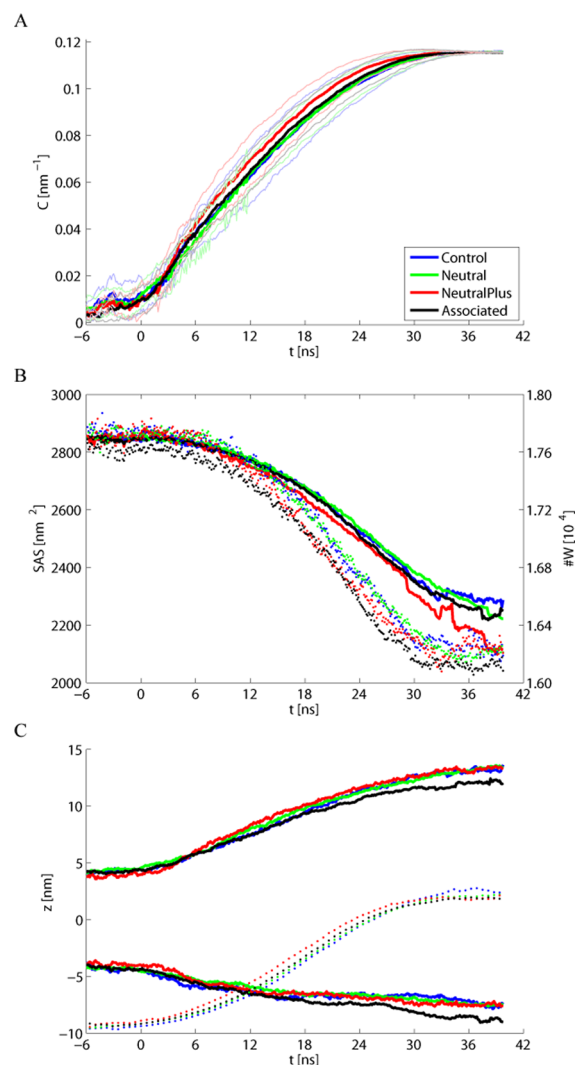


**Figure 4.** Averages for the different simulation series plotted against the simulation time, showing (A) the membrane curvature, including standard deviations indicated by the lighter colored lines. (B) The solvent accessible surface (left y-axis) and the number of waters within 1.2 nm of the membrane (right y-axis). (C) Full lines represent the minimal and maximal z-coordinates of the fatty acids; the dotted lines represent the average z-coordinates of those water particles that are encapsulated at the end of the simulation, with the trajectory of each particle retraced from the final frame to correct for movement across the periodic boundaries. Here, the z-coordinate is calculated as the distance along the membrane normal from the center of mass of the membrane at  $t = 0$  ns.

acids as a function of the simulation time, where all simulation boxes were rotated, when needed, such that the membrane closes in the downward direction. Rather than folding its sides downward to enclose a certain volume of water, the center of the membrane appears to bulge upward. This is necessarily followed by an influx of solvent to fill the space that is emptied by the membrane, as demonstrated by the upward motion of the average z-coordinates of the finally encapsulated water particles shown in Figure 4C as well. Figure 4B shows that the amount of water molecules within 1.2 nm of the membrane decreases steadily as the curvature of the vesicle increases. This decrease in the amount of water molecules near the membrane coincides with a decrease in the solvent accessible surface, as calculated using MSMS<sup>32</sup> with a probe size of 1.0 nm. Again,

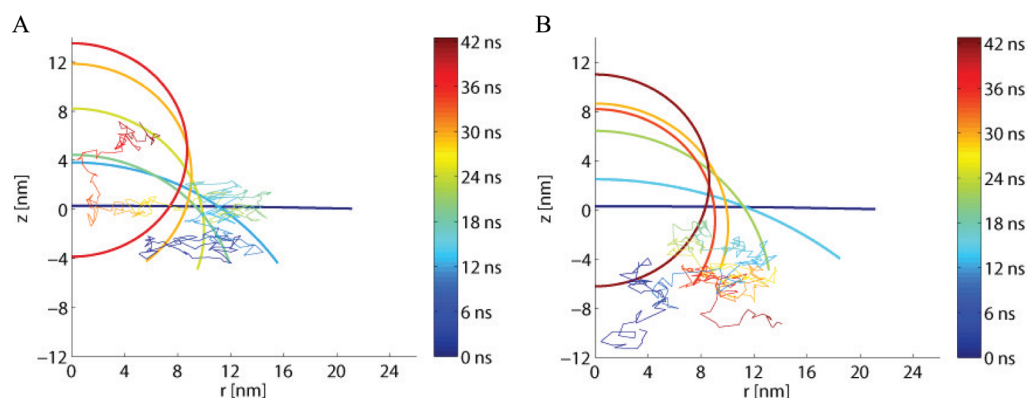


**Figure 5.** Selected protein trajectories from the Associated (A) and the NeutralPlus (B) series. On the horizontal axis, the distance  $r$  to the axis normal to the membrane and through its center of mass is shown, whereas on the vertical axis the  $z$ -coordinate is given. The protein trajectory is shown as a continuous line, whereas a partial spherical surface is used as a schematic representation of the curved membrane. The colors represent the simulation time, with dark blue for the start of the simulation, which changes into green, yellow, and eventually red at the end of the simulation. Importantly, due to variations of the curvature in different parts of the membrane, there are still significant variations to the schematic representation present in the actual configurations, especially in the first half of the simulation.

this result is independent of the presence of the model proteins as well as of the protein–membrane interaction.

The diffusion of one typical protein from the “Associated” series that is encapsulated by the forming vesicle is shown in Figure 5A. A representation of the different stages of closure of the vesicle is included as a spherical fit of the membrane coordinates. It can be seen from this representation that the protein diffusion is restricted once it is within the closing vesicle, after 25 ns in this case. Due to the attractive interaction between the protein and the membrane in this simulation, the protein is drawn into the closing vesicle. In the Neutral and NeutralPlus series, this specific attraction is not present, so proteins that enter the closing vesicle freely diffuse out of the forming vesicle again, as shown by the typical example in Figure 5B.

## DISCUSSION AND CONCLUSION

Using molecular dynamics simulations, we have investigated protein crowding in the spontaneous formation of model vesicles. In our previous work, it was already discussed that entropy is the driving force behind the bilayer–vesicle transition.<sup>4</sup> The current results in Figure 4A and B are in good agreement with those earlier results and show no significant difference in the vesicle formation between the four different series, indicating that the presence of the solvated model proteins does not have a significant effect on the driving force behind the vesicle formation. Moreover, the simulations show a reduced concentration of proteins inside the spontaneously formed vesicles, while this concentration could be increased well above the bulk concentration, by means of an attractive interaction between the membrane surface and the proteins.

The simulations of the bilayer–vesicle transition demonstrate that, rather than folding the edge of the membrane downward to enclose a certain volume of water, the center of the membrane appears to bulge upward, which is accompanied by the influx of solvent. This “bilayer bulging” pathway could explain the lower-than-expected concentration of proteins in the Neutral and NeutralPlus series. As the influx of solvent in the “bulging” phase depends on the rate of diffusion, it is likely that the small water molecules diffuse inward more easily than the bulkier protein molecules. In the absence of additional

forces to drive the proteins inward, such as an enlarged protein–membrane interaction, this leads to a reduced average protein concentration inside the vesicles. Lower diffusion speed is expected to lead to a lower protein concentration inside the vesicle. As the diffusion rate of a protein depends on its size, we expect that our proposed mechanism should result in encapsulated concentrations of larger proteins that are lower than those of smaller proteins. Therefore, it is interesting to note that Dominak et al. have recently reported similar findings in experiments encapsulating large biomacromolecules poly-(ethylene glycol) or dextran.<sup>15</sup> In their experiments, they have found essentially equal internal and external concentrations of labeled biomacromolecules with a hydrodynamic radius smaller than 10 nm, whereas the internal concentrations were reduced significantly for solutes larger than 10 nm. It would be interesting to systematically investigate the effect of protein size, as well as shape, on the encapsulated protein concentration in vesicle formation. Our generic protein model could be used to do this in molecular simulations, where both the size and the shape of the proteins can be adjusted without changing any of the interaction parameters. However, this is beyond the scope of the current work.

Due to the “bilayer bulging” in the bilayer–vesicle transition, the encapsulated protein concentration in vesicles depends on two phenomena: the inward diffusion of proteins along with the water that fills up the vesicle and adhesion of proteins to the interior surface of the membrane. In the former phenomenon, the diffusion rate of the proteins is important, whereas, in the latter, the protein–membrane interaction determines how many proteins are encapsulated. The effect of vesicle size on these mechanisms has not been investigated in this work. However, it is expected that the vesicle size mainly affects the encapsulation efficiency due to protein–membrane adhesion, since with adhesion the amount of encapsulated proteins is dependent on the membrane area, or the square of the vesicle radius. Therefore, the effect of the second mechanism would be a positive correlation of the protein concentration with the area divided by the volume of the vesicle, i.e., the concentration to be inversely proportional to the radius of the vesicle. In experiments encapsulating ribosomes in liposomes, Pereira de Souza et al. find that the relationship between the internal ribosome concentration  $C$  and the liposome radius  $r$  can be

described by a power function of the form  $C = (3.5 \pm 0.5)/r^{1.28 \pm 0.04} \mu\text{M}$ .<sup>17</sup> The radii of these experimental vesicles are far larger than what we can deal with in our simulations, prohibiting a direct comparison. Although the agreement with our expectations in size dependence is reasonable, the experimental findings may also indicate a more complex behavior.

The experimental results reported by Luisi et al.,<sup>16</sup> for instance, also show the coexistence of superfilled and empty vesicles and a power law distribution of the enclosed protein concentrations. Although we do observe both empty and superfilled vesicles in our simulations (Figure 3), the data size by which these histograms have been obtained is too small to draw conclusions about the distributions. The protein crowding observed experimentally may be caused by other factors, such as an entropic effect or a slow-down of the vesicle formation. Further systematic research on the effect of a slow-down of the vesicle formation, for instance, by changing the vesicle size or by employing different protein–membrane interactions or more realistic protein models, might shed more light on the underlying mechanisms.

To obtain feasible computation costs, the vesicle size and the system size have to be much smaller than those of experimental systems, and the protein concentration is higher. Since we are interested in the underlying mechanisms, we have designed a small generic protein model. To limit the degrees of freedom, we use a spherical protein composed of particles with a single interaction type, which allows systematic variation of the protein–membrane interactions. Moreover, for the same reason, we have used very generic molecules in our model, such as the water particles where the effects of solute and ion interactions are included implicitly. In Figure 4, we have shown that our model proteins do not affect the bilayer–vesicle transition. Therefore, in our simulations, we investigate the effect of an increase of the protein–lipid interaction *ceteris paribus*. That proteins do not affect the bilayer–vesicle transition in the experimental systems is, however, not unambiguous. It would therefore be interesting to study also the influence of other model proteins on the bilayer–vesicle transition, for instance, proteins of different size or shape as well as proteins with different chemical character, such that they, for instance, (partially) insert into the membrane. Given the abstractions in the model, the simulations are not intended to represent one particular experimental system. The strength of the approach presented here is in its genericity, presenting mechanisms and insights which may inspire experimentalists to design new experiments.

Our findings suggest that it is possible to achieve an enhanced encapsulation of solutes, such as proteins or nucleic acids, inside spontaneously formed lipid vesicles, by means of an attractive force between the membrane and the solute. This could be achieved by a specific molecular interaction between one of the constituents of the membrane and (a section of) the solute's surface. Another possibility is an electrostatic attraction between the negatively charged membrane surface and positively charged amino acids in the protein sequence, or, indirectly, with negatively charged amino acids through positively charged counterions.<sup>33</sup> To test the effect of the protein–membrane interaction experimentally, one could consider using a combination of a membrane and a protein or peptide where the protein–membrane interaction is tunable, e.g., by changing the pH or the salt concentration; for example,

arginine-6 might be used as a protein model, combined with an oleic acid membrane.

Efforts to design artificial cells could benefit from the new insights provided by this work. A focus on the solute–membrane interactions in the early stages of template design could facilitate the development of liposomes with high protein, or RNA, content. A possible application is the design of liposomes that encapsulate an entire RNA transcription and translation machinery, as reported by Pereira de Souza and co-workers.<sup>17</sup> In view of the large number of required building blocks of such a machinery, it would be beneficial to choose the membrane components and other variables like the pH, such that the membrane surface has a strong attractive interaction with the quintessential elements for RNA replication.

Enhanced encapsulation of proteins inside the vesicles has been achieved in our simulations by means of an attractive interaction between the membrane surface and the proteins, whereas the interior protein concentration is lower than that of the solution in the absence of such a specific attraction. These results indicate that an attractive interaction between proteins and the membrane surface is a plausible explanation for protein crowding. Moreover, in our simulations, we observe a “bilayer bulging” pathway in the bilayer–vesicle transition. These findings could be valuable in the design of artificial cells. Further research remains necessary to explain experimentally observed power law distributions in enclosed proteins as well as the coexistence of superfilled and empty vesicles. Furthermore, the molecular model presented here could be used to systematically investigate the effect of the vesicle size, as well as the role of the shape and size of the proteins in the observed protein crowding.

## ■ ASSOCIATED CONTENT

### 📄 Supporting Information

An overview of the force field used and of the interaction parameters is provided. Furthermore, the calculation of the membrane curvature is discussed. This material is available free of charge via the Internet at <http://pubs.acs.org>.

## ■ AUTHOR INFORMATION

### Corresponding Author

\*E-mail: [p.a.j.hilbers@tue.nl](mailto:p.a.j.hilbers@tue.nl).

### Notes

The authors declare no competing financial interest.

## ■ ACKNOWLEDGMENTS

B.v.H. acknowledges financial support from the Dutch National Research School Combination Catalysis Controlled by Chemical Design (NRSC-Catalysis).

## ■ REFERENCES

- (1) Helfrich, W. Z. *Naturforsch., C* **1973**, *28*, 693–703.
- (2) Fromherz, P. *Chem. Phys. Lett.* **1983**, *94*, 259–266.
- (3) Leng, J.; Egelhaaf, S.; Cates, M. *Biophys. J.* **2003**, *85*, 1624–1646.
- (4) Markvoort, A.; Pieterse, K.; Steijjaert, M.; Spijker, P.; Hilbers, P. J. *Phys. Chem. B* **2005**, *109*, 22649–22654.
- (5) Wang, Z.; He, X. J. *Chem. Phys.* **2009**, *130*, 094905.
- (6) Gummel, J.; Sztucki, M.; Narayanan, T.; Gradzielski, M. *Soft Matter* **2011**, *7*, 5731–5738.
- (7) Szostak, J. *Philos. Trans. R. Soc., B* **2011**, *366*, 2894–2901.
- (8) Meierhenrich, U.; Filippi, J.; Meinert, C.; Vierling, P.; Dworkin, J. *Angew. Chem., Int. Ed.* **2010**, *49*, 3738–3750.

- (9) Stano, P.; Carrara, P.; Kuruma, Y.; de Souza, T. P.; Luisi, P. J. *Mater. Chem.* **2011**, *21*, 18887–18902.
- (10) Takinoue, M.; Takeuchi, S. *Anal. Bioanal. Chem.* **2011**, *400*, 1705–1716.
- (11) Noireaux, V.; Maeda, Y.; Libchaber, A. *Proc. Natl. Acad. Sci. U.S.A.* **2011**, *108*, 3473–3480.
- (12) Kurihara, K.; Tamura, M.; Shohda, K.; Toyota, T.; Suzuki, K.; Sugawara, T. *Nat. Chem.* **2011**, *3*, 775–781.
- (13) Chen, I.; Roberts, R.; Szostak, J. *Science* **2004**, *305*, 1474–1476.
- (14) Tsai, F.; Stuhmann, B.; Koenderink, G. *Langmuir* **2011**, *27*, 10061–10071.
- (15) Dominak, L.; Omiatsek, D.; Gundermann, E.; Heien, M.; Keating, C. *Langmuir* **2010**, *26*, 13195–13200.
- (16) de Souza, T. P.; Stano, P.; Luisi, P. *ChemBioChem* **2009**, *10*, 1056–1063.
- (17) de Souza, T. P.; Steiniger, F.; Stano, P.; Luisi, P. *ChemBioChem* **2011**, *12*, 2325–2330.
- (18) Luisi, P.; Allegretti, M.; de Souza, T. P.; Steiniger, F.; Fahr, A.; Stano, P. *ChemBioChem* **2010**, *11*, 1989–1992.
- (19) Marrink, S.; de Vries, A.; Tieleman, D. *Biochim. Biophys. Acta, Biomembr.* **2009**, *1788*, 149–168.
- (20) Markvoort, A.; Marrink, S. *Curr. Top. Membr.* **2011**, *68*, 259–294.
- (21) Yang, K.; Ma, Y. *Soft Matter* **2012**, *8*, 606–618.
- (22) Noguchi, H.; Takasu, M. *Phys. Rev. E* **2001**, *64*, 41913–41920.
- (23) Yamamoto, S.; Maruyama, Y.; Hyodo, S. *J. Chem. Phys.* **2002**, *116*, 5842–5850.
- (24) Marrink, S.; Mark, A. *J. Am. Chem. Soc.* **2003**, *125* (49), 15233–15242.
- (25) de Vries, A.; Mark, A.; Marrink, S. *J. Am. Chem. Soc.* **2004**, *126* (14), 4488–4489.
- (26) Risselada, H.; Mark, A.; Marrink, S. *J. Phys. Chem. B* **2008**, *112* (25), 7438–7447.
- (27) Smeijers, A.; Pieterse, K.; Markvoort, A.; Hilbers, P. *J. Phys. Chem. B* **2006**, *110*, 13212–13219.
- (28) Markvoort, A.; Spijker, P.; Smeijers, A.; Pieterse, K.; van Santen, R.; Hilbers, P. *J. Phys. Chem. B* **2009**, *113*, 8731–8737.
- (29) Smeijers, A.; Pieterse, K.; Markvoort, A.; Hilbers, P. *J. Phys. Chem. B* **2006**, *110*, 13614–13623.
- (30) Spijker, P.; van Hoof, B.; Debertrand, M.; Markvoort, A.; Vaidehi, N.; Hilbers, P. *Int. J. Mol. Sci.* **2010**, *11*, 2392–2420.
- (31) Markvoort, A.; Pfleger, N.; Staffhorst, R.; Hilbers, P.; van Santen, R.; Killian, J.; de Kruijff, B. *Biophys. J.* **2010**, *99*, 1520–1528.
- (32) Sanner, M.; Spehner, J.-C.; Olson, A. *Biopolymers* **1996**, *38*, 305–320.
- (33) Mulgrew-Nesbitt, A.; Diraviyam, K.; Wang, J.; Singh, S.; Murray, P.; Li, Z.; Rogers, L.; Mirkovic, N.; Murray, D. *Biochim. Biophys. Acta, Mol. Cell Biol. Lipids* **2006**, *1761*, 812–826.